ACS APPLIED MATERIALS & INTERFACES

RESEARCH ARTICLE

www.acsami.org

Magnesium and Calcium Organophyllosilicates: Synthesis and In vitro Cytotoxicity Study

Hyo-Kyung Han,[†] Young-Chul Lee,[‡] Moo-Yeol Lee,[†] Avinash J. Patil,[§] and Hyun-Jae Shin*[,‡]

[†]College of Pharmacy, Dongguk University, Pil-dong, 3-ga, Jung-gu, Seoul, Republic of Korea

[‡]Department of Chemical and Biochemical Engineering, Chosun University, Republic of Korea

[§]Centre For Organized Matter Chemistry, School of Chemistry, University of Bristol, Bristol BS8 1TS, United Kingdom

Supporting Information

ABSTRACT: Synthesis of multifunctional hybrid nanomaterials for biomedical applications has received great attention. Herein, we examine the potential toxicity of organophyllosilicates on cells from different organs such as A549 (lung epithelial cancer), HT-29 (colon epithelial cancer), MRC-5 (lung fibroblast) and CCD-986sk (skin fibroblast) cells. For this, aminopropyl functionalized magnesium phyllosilicate (AMP clay) and aminopropyl functionalized calcium phyllosilicate (ACP clay) were prepared using one-pot direct sol−gel method. Toxic effects of these organoclays on normal fibroblast and tumor cells were examined under varying concentrations and exposure times. MTT and LDH assays indicated that both organoclays had little cytotoxicity in all of the cells tested at concentrations as high as 500 μg/mL. Even at high concentration (1000 μg/mL), the toxicity of both organoclays on cell viability and membrane damage was not severe and appeared to be cell type specific. In addition, organoclays did not induce apoptosis at concentrations as high as 1000 μg/mL.

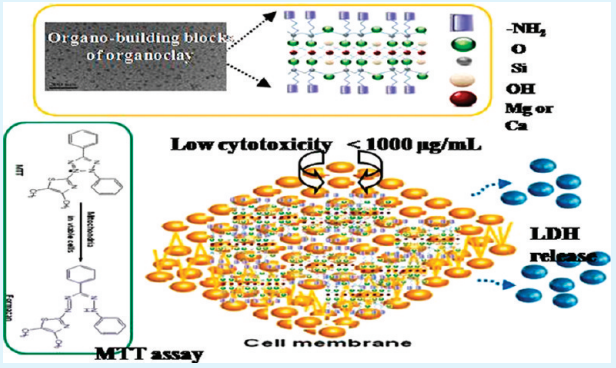

KEYWORDS: phyllosilicate, organoclay, nanomaterials, cytotoxicity, apoptosis, cell type

1. INTRODUCTION

Recent advances in self-organized assemblies of organic and inorganic materials in nanotechnology are of growing interest because self-assembled cage structures made of clay materials can be used as constrained environments for the encapsulation of guest molecules with potential applications in sensing, catalysis, electronics/optics, and environmental cleanup.[1,2] Among numerous nanoscale self-assembled structures, there have been many reports on the synthesis and characterization of organically modified derivatives of phyllosilicate (organoclays) because of their wide applicability as adsorbents of toxic contaminants, paints, cosmetics, and drug delivery.[3−7] Taken together, the interaction of human with biological and environmental systems to generate the toxicity of nanomaterials including nanoclays is significantly necessitated.[8−10]

To date, the cytotoxicology of nanoparticles such as silica, semiconductors, nanoscale zerovalent iron, quantum dots, and halloysite clay[9,11−19] as well as the surface modification or functionalization of nanomaterials to reduce their cytotoxic effects[20−24] have been investigated. For silicate nanoclay, the toxicity for nanosilicate platelets (NSP) derived from natural montmorillonite clay has been recently published.[25] However, toxicological effects of nanomaterials upon humans and the environment are still unknown. Therefore, as the ability to mass produce functional nanomaterials grows, understanding and administration of their toxic effects is equally important. As a representative, 3-aminopropyl functionalized phyllosilicates (organoclays) have not received much attention even though nanocomposites of organoclay with polymers have been successfully prepared for drug release in batch experiments.[7] The use of these organoclays has focused on hybrid nano-object and nanostructure wrapping biomolecules;[2,26−33] organic−inorganic nanocomposites and nanohybrid materials by covalent bonding with fluorescein isothiocyanate (FITC),[34] and shift base using AMP clay's cationic building blocks in water media.[35] Recent studies have shown that organically modified magnesium phyllosilicates can be used to produce a range of functional bioinorganic nanocomposites for biocatalysis and controlled drug release.

The artificial amine functional group on phyllosilicate organoclays was produced by employing copolymerization of organotrialkoxysilanes in the presence of metallic ions. This resulted in nanocomposites with layered lamella structures. An interesting feature associated with these inorganic layered compounds is connected to the existence of organophilic functionalities distributed in the interlayer cavities.[1,2,26−28] These hybrid materials are members of a family of 2:1 organo-modified trioctahedral phyllosilicates whose structures are similar to those found in natural talc, formulated as $[H_2N(CH_2)_3]_8[Si_8Mg_6O_{16}(OH)_4]$.[29,30,34] The

Received: April 5, 2011
Accepted: May 25, 2011
Published: May 25, 2011

Table 1. Name and Types of Cell Lines Tested in This Study

cell name	origin	tissue	cell morphology	histopathology
CCD-986sk	*Homo sapience* (human)	skin	fibroblast	normal
A549	*H. sapience* (human)	lung	epithelial	carcinoma
MRC-5	*H. sapience* (human)	lung	fibroblast	normal
HT-29	*H. sapience* (human)	colon	epithelial	carcinoma

major advantage of this synthesis is that it is a one-step direct synthesis, wherein all reactions occur in ambient conditions. Functionalized magnesium phyllosilicate (AMP clay) is increasingly used in materials research because of its high density of amine groups covalently attached to a backbone of metal cationic ions and its water-solubility.[2,7,26−28] Furthermore, it has potential as a nanoadsorbent for wastewater treatment or as a nonviral vector that can be used for encapsulating proteins or for gene transfer.[34]

Consequently, it is conceivable that organoclay nanomaterials may be exposed to the environment, or they may be administered into the human body through oral, pulmonary, or transdermal delivery. With respect to in vivo and field applications, the toxicity and health effects of these nanomaterials are of great concern. Therefore, to prevent potential hazards caused by human and environmental exposure to organoclays, their toxicological effects need to be clearly defined. The information regarding their safety profiles in different tissues and organs is of vital importance to the future application of organoclays as a biomaterial. In the present study, organoclays with different cations (Mg and Ca) were synthesized, and their potential toxicity was examined using cells from different organs with varying concentrations and duration of exposure. Such a toxicological study can not only provide critical information about the biological applications of organoclays but can also help to avoid any undesirable effects.

2. MATERIALS AND METHODS

2.1. Materials and Cells. 3-Aminopropyltriethoxysilane (APTES, 99%) and paclitaxel were purchased from Sigma-Aldrich (St. Louis, MO, USA). Ethanol (>99.9%) was purchased from Merck KGaA (Darmstadt, Germany). Magnesium chloride hexahydrate (98.0%) and calcium chloride dehydrate (80%) were obtained from Junsei Chemical Co., Ltd. (Tokyo, Japan). 5-(and-6)-Carboxy-2′,7′-difluorodihydrofluorescein diacetate (carboxy-H_2DFFDA) and MTT (3-(4,5-dimethylthiazol-2-yl)-2,5-diphenyltetrazolium bromide) were purchased from Invitrogen Co. (Carlsbad, CA, USA) and Sigma-Aldrich Co. (St. Louis, MO, USA), respectively. Fetal bovine serum (FBS), cell culture media, antibiotics, and all other reagents used in cell culture studies were purchased from Seolin Science Co. (Seoul, Korea). A549 (lung epithelial cancer), HT-29 (colon epithelial cancer), MRC-5 (lung fibroblast), and CCD-986sk (skin fibroblast) cells were obtained from the Korean Cell Line Bank (Seoul, Korea) (Table 1). Cells were routinely maintained in RPMI 1640 (A549 and HT-29 cells), Dulbecco's Modified Eagle's Medium (DMEM) (CCD-986sk cells) or Minimal Essential Medium (MEM) (MRC-5 cells). All media were supplemented with 10% FBS and penicillin (50 IU/mL)/streptomycin (50 μg/mL). All cells were maintained in an atmosphere of 5% CO_2 and 90% relative humidity at 37 °C. The distilled deionized water (ddH_2O) used in this study was purified using an EASYpure water purification system (Barnstead, USA) and had an initial resistivity of 18.3 MΩ·cm.

2.2. Synthesis of Organoclays. Typically, aminopropyl-functionalized magnesium (AMP) and calcium (ACP) organophyllosilicate clay was prepared at room temperature by the dropwise addition of 3-aminopropyltriethoxysilane (1.3 mL, 5.63 mmol) to an ethanolic solution of magnesium chloride (0.84 g, 8.82 mmol) and calcium chloride (0.979 g, 8.82 mmol) in ethanol (20 g).[30,34] The white slurry obtained after 5 min was stirred overnight, and the precipitate was isolated by centrifugation, washed with ethanol (50 mL) and dried at 40 °C. The molar ratio of Mg and Ca to Si was ca. 0.75.

2.3. Characterization of the Synthesized Clays. Morphological characterization of AMP and ACP clays was performed by transmission electron microscopy (TEM) (JEM-2100F, JEOL Ltd.) and scanning electron microscopy (SEM) (Sirion) with ED(A)X elemental analysis. The particle size distribution of clays in aqueous solution was examined by dynamic laser scattering (DLS) particle size (HELOS/RODOS & SUCELL, Germany). Powder X-ray diffraction (PXRD) patterns of the clays were assessed on a RIGAKU D/MAX-IIIC (3 kW) with Cu Kα radiation (Tokyo, Japan). FT−IR spectra were collected on a NICOLET 6700 (Thermo Fisher Scientific, Inc., Waltham, MA, USA). Each spectrum, recorded as the average of 32 scans with a resolution of 4 cm^{-1}, was collected from 4000 to 450 cm^{-1} in pellet mode.

2.4. Effect of Organoclays on Cell Viability. The effect of synthesized organoclays (AMP and ACP clay) on cell viability was assessed using a 3-(4,5-dimethylthiazol-2-yl)-2,5-diphenyl tetrazolium bromide (MTT) assay. Cells were seeded into 48-well plates at a concentration of 9×10^4 cells per well. After 24 h, cells were treated with organoclays (10−1000 μg/mL) for an additional 24 h. In the case of time-dependent studies, cells were incubated with 1000 μg/mL of organoclays for 24, 48, and 72 h. Next, cells were treated with 0.5 mg/mL MTT for 3 h to form insoluble dark blue formazan crystals. At the end of the incubation, the formazan crystals were dissolved in DMSO, and the absorbance at 570 nm was measured with a VersaMax microplate reader (Molecular Devices, CA, USA).

2.5. LDH Assay. Lactate dehydrogenase (LDH) release was monitored with the CytoTox-ONE^{TM} homogeneous membrane integrity assay (Promega). Cells (2×10^3/well) were seeded in a 96-well plate and, after 24 h, were incubated with AMP clays (0.5−1000 μg/mL) for 24, 48, and 72 h. The medium (100 μL) was then harvested and placed in new microtiter plates. Finally, 100 μL of substrate solution was added to each well and incubated for 10 min at room temperature. Next, stop solution (50 μL) was added to each well, and the fluorescence intensity was immediately measured with a SpectraMax M2 (Molecular Devices, CA, USA) at an excitation wavelength of 560 nm and an emission wavelength of 590 nm. Cytotoxicity is expressed relative to basal LDH release by untreated control cells.

2.6. Apoptosis Assay. Apoptotic cells were detected by the Vybrant apoptosis assay kit (Molecular Probes, Eugene, OR, USA), which employed annexin V to detect phosphatidylserine exposure, according to the manufacturer's instructions. After a 24-h treatment of AMP and ACP clays (100−1000 μg/mL), cells were stained with Alexa Fluor 488-conjugated annexin V and propidium iodide (PI), a membrane impermeable nucleic acid binding dye. Cells were imaged with a Nikon Ti−U inverted microscope equipped with a CFI Plan Apochromat 20× objective lens (Nikon, Melville, NY, USA) and a Luca EMCCD Camera (Andor Technology, Belfast, Ireland). Illumination was provided with a Lambda DG-4 wavelength switcher with a xenon arc lamp (Sutter Instruments, Novato, CA, USA). Excitation/emission wavelengths used for Alexa Fluor 488 and PI were 480/535 nm and 540/605 nm, respectively. Images were acquired and analyzed with a Meta Imaging System (Molecular Devices, West Chester, PA, USA). Experiments were repeated three times, and representative images are presented.

2.7. Statistical Analysis. All of the means obtained are presented with their standard deviation. Statistical analyses were carried out using one-way ANOVA with Dunnett's posthoc test. A p value <0.05 was considered as statistically significant.

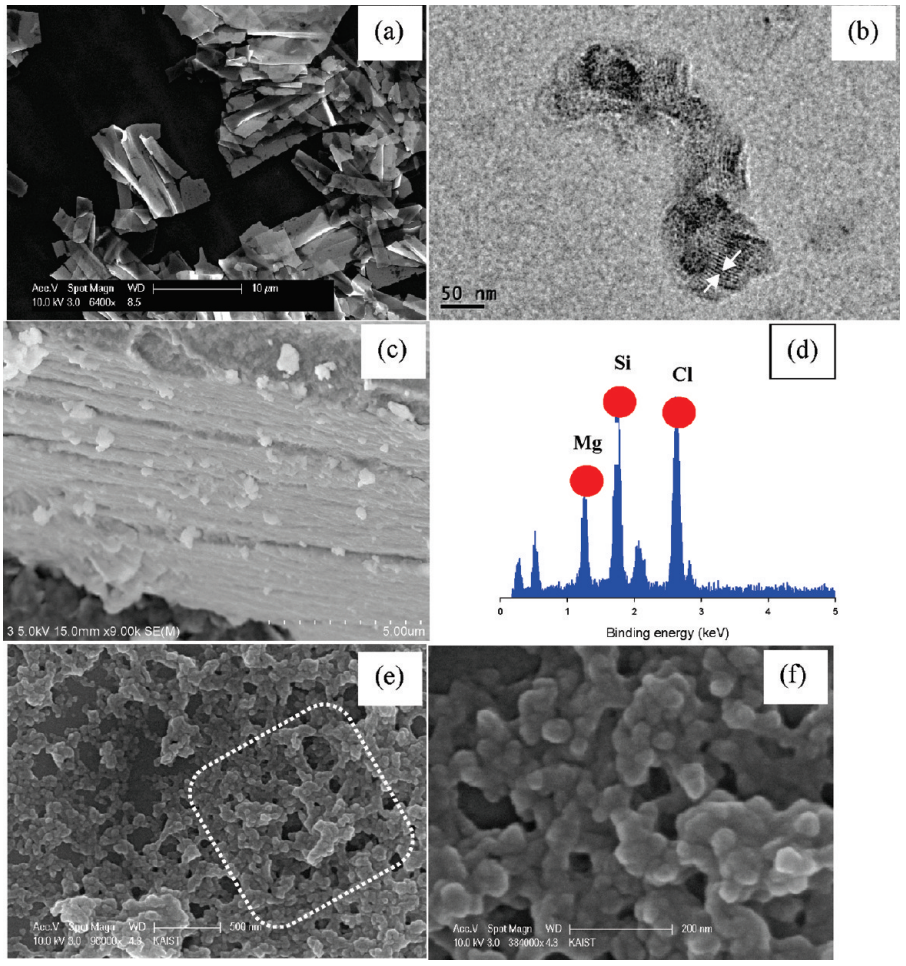

Figure 1. (a) SEM image and (b) TEM image of AMP clay in ethanol (2.5 mg/mL). (c) SEM image of powder AMP clay and energy dispersive X-Ray (EDX) analysis of AMP clay. The remaining peaks of elemental composition are C, O, and Pt. (e) Low- and (f) high-magnification of a SEM image of ACP clay in ethanol (5 mg/2 mL). Note: AMP and ACP clays indicate aminopropyl functionalized magnesium phyllosilicate and aminopropyl functionalized calcium phyllosilicate, respectively.

3. RESULTS AND DISCUSSION

3.1. Screening of Organoclays and Structure Determination. Theoretically, numerous organic clays could be synthesized by the combination of various silane compounds and metal chlorides. We have checked the various organoclays described in the literature: phyllosilicate frameworks as cationic metals and functional groups of organic moieties as APTES or amine-related compounds.[1] APTES (ca. pH 10.5) in metal cation solutions did not require an acid/base catalyst, indicating that reaction was autocatalytic and the reaction product was a white precipitate at room temperature. Among phyllosilicate above-mentioned, we have chosen AMP and ACP clay as model compounds for this toxicity study after preliminary toxicity screening using MTT assays, because nickel and zinc are known to be toxic ions. AMP clay sheets were stacked in ethanol and partially protonated with aminopropyl side chains, and they displayed macroscale organo-building. The size of the AMP nanoparticles was polydispersed at ~50 nm or larger in the microsize range in ethanol, which was a typical layered clay structure (Figure 1a−c). In particular, the edge-view of the AMP clay exhibited a lamellar (regular layered) structure, with the layers spaced about 2 nm apart (Figure 1b). As shown in images e and f in Figure 1, ACP clay also exhibited a spherical grape-like inorganic−organic hybrid, as observed in the SEM images. In addition, images e and f in Figure 1 show the significant intralayer disorder due to broader reflections. This result was compared with that obtained for calcium organosilicate hybrids with triethoxysilane (TES) precursors.[36] In EDX elemental analysis, compositions of Mg (or Ca), Si and Cl were predominantly detected (Figure 1d). Ca ions were detected at a 3.71 keV binding energy. The chloride ions were stabilized by surrounding positive ammonium ions. In addition, we investigated the particle size distribution in aqueous media of AMP and ACP clays when considering cellular uptake (Figure 2). These examination showed that X_{10}, X_{50}, and X_{99} (the cumulative particle size at 10, 50, and 99%) of AMP and ACP clays represent 35.86/44.31/64.60 nm and 73.51/93.35/143.08 nm. The surface and volume mean diameter of AMP and ACP clays are 43.74/44.93 nm and 91.80/94.99 nm. To further investigate protonated and exfoliated organoclays, we performed visual checks for optical transparency after a 5 min sonication in ddH_2O with an increase in pH (ca. 10.5). PXRD profiles of the as prepared AMP and ACP clays revealed a low angle interlayer d_{001} reflections at 1.55 and 1.38 nm respectively, which is slightly less than that obtained in the previous report (1.86 nm).[28] In the case of AMP clay, broad peaks at d_{002} = 0.82 nm (2θ = 10.81), $d_{020,110}$ = 0.40 nm (2θ = 22.33), $d_{130,200}$ = 0.25 nm (2θ = 35.37), and $d_{060,330}$ = 0.16 nm (2θ = 59.29), with an

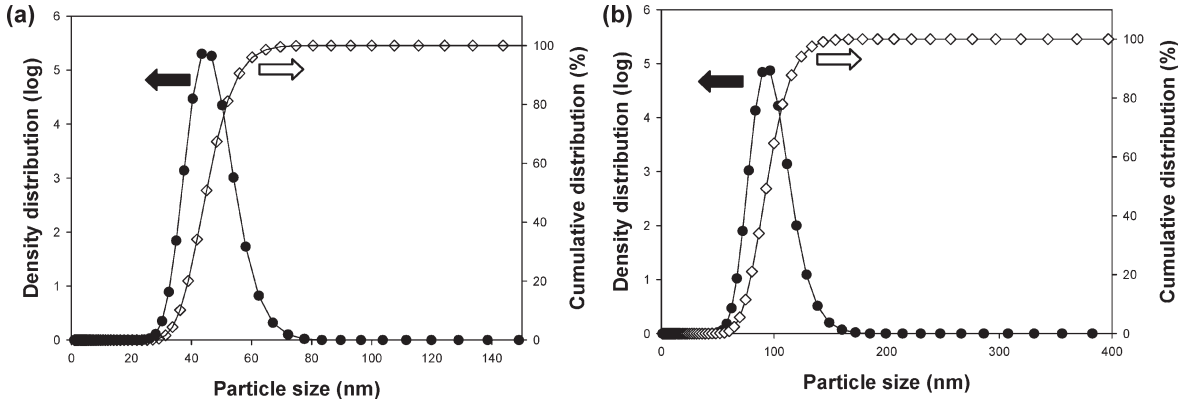

Figure 2. Particle size distribution of AMP clay (a) and ACP clay (b) by dynamic light scattering (DLS) analysis. Note: Red and blue arrows stand for the density and the cumulativeness of probability sizes, respectively.

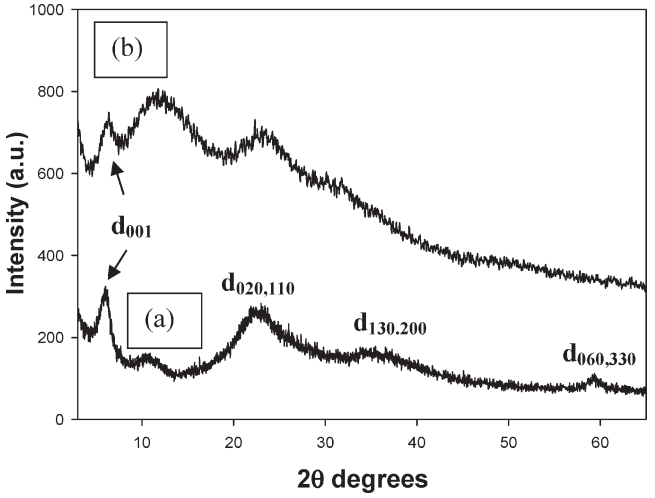

Figure 3. PXRD patterns of (a) AMP clay and (b) ACP clay. Arrow marks indicate the basal spacing.

intraplane d_{060} smectite reflection at 2θ = 59.29° (Figure 3a), indicated that the basic unit of the AMP clay structure was retained. Assuming that in-plane reflections (the broad higher angle region) at 31.7 and 50.1° are assigned to (130, 200) and (060, 330), ACP clay showed similar characteristics of 2:1 trioctahedral phyllosilicate, corresponding to a reported result.[36] However, based on weak in-plane reflections of ACP clay, the disorder of the inorganic portion of the organoclay seemed to correspond to the SEM morphology (Figure 1e,f). Furthermore, in the FT-IR spectra (see the Supporting Information, Figure S1), the AMP and ACP clay materials showed vibration modes for Mg−O (559 cm^{-1}) and Ca−O (589 cm^{-1}) respectively. The peaks observed for CH_2 (3,000 cm^{-1}), OH (3,384 cm^{-1}), Mg−O−Si (849 cm^{-1}), Si−O−C (849 cm^{-1}), Si−OH (1,034 cm^{-1}), and Si−O−Si (1,130 cm^{-1}) were in good agreement with earlier reports.[34]

3.2. Cellular Toxicity of Organoclay. The potential toxicity of synthesized organoclays was evaluated using cultured cancer cells and normal cells from different organs at various concentrations in terms of cell viability, membrane damage, and apoptosis. Because organoclays have attracted much attention as drug delivery nanocarriers for biological purposes, the assessment of their potential toxicity should be critical to expanding their application to the development of effective drug delivery systems. To examine cellular toxicity, we selected four different cell lines (human lung cancer A549 cells, human lung fibroblast MRC-5 cells, human colon cancer HT-29 cells and human skin fibroblast CCD-986sk cells) for the present study. These cell lines include normal pulmonary and dermal fibroblast cells as well as tumor cells of the colon and lung, to assess the cytotoxicity of organoclays in potential dermal and pulmonary contacts or in future applications as a drug delivery carrier for different administration routes (oral/pulmonary/transdermal). In addition, these lines were used to compare the cytotoxicity of organoclays in cancer cells and normal cells.

As shown in Figure 4, the effects of organoclays on cell viability and proliferation were measured using the MTT assay, which is based on the reduction of the yellow tetrazolium salt MTT by metabolically active cells, resulting in purple formazan crystals. Neither AMP nor ACP clays showed any toxic effect on cell viability for the entire cell lines tested, except A549 cells, over the concentration range of 10−1000 μg/mL (Figure 4a). In the case of A549 cells, only at a concentration of 1000 μg/mL did both organoclays tend to block cell viability. In addition, the cytotoxicity of the organoclays was not time-dependent and maintained a low toxicity as the incubation time increased up to 72 h (Figure 4b). These results suggested that AMP and ACP clays should have little toxicity on the proliferation or viability of cells.

Cell membrane damage induced by organoclays was also monitored by the LDH leakage assay, as LDH can leak into the extracellular fluid only after membrane damage.[37] As shown in Figure 5, AMP clays were not cytotoxic at concentrations as high as 1000 μg/mL in all tested cell lines except CCD986sk cells, implying that its toxicity may be cell type specific. Currently, the mechanism for the cell-type specific toxicity of nanoparticles is not clearly defined yet. However, there have been some reports that cytotoxicity of nanoparticles can be variable depending on cell types,[38,39] although underlying mechanism may be different depending on the characteristics of nanomaterials. Assuming the cytotoxicity of AMP can be mediated by oxidative stress through the generation of reactive oxygen species like other types of nanoclay,[40] the most critical determinant of cytotoxicity will be the antioxidant capacity which may be variable depending on cell types, resulting in the cell-type specific cytotoxicity. Compared to the control group, AMP clay showed a statistically significant increase in LDH release in CCD986sk cells over a concentration range of 500−1000 μg/mL. However, considering that this increase is still less than 20%, AMP clay is unlikely to cause

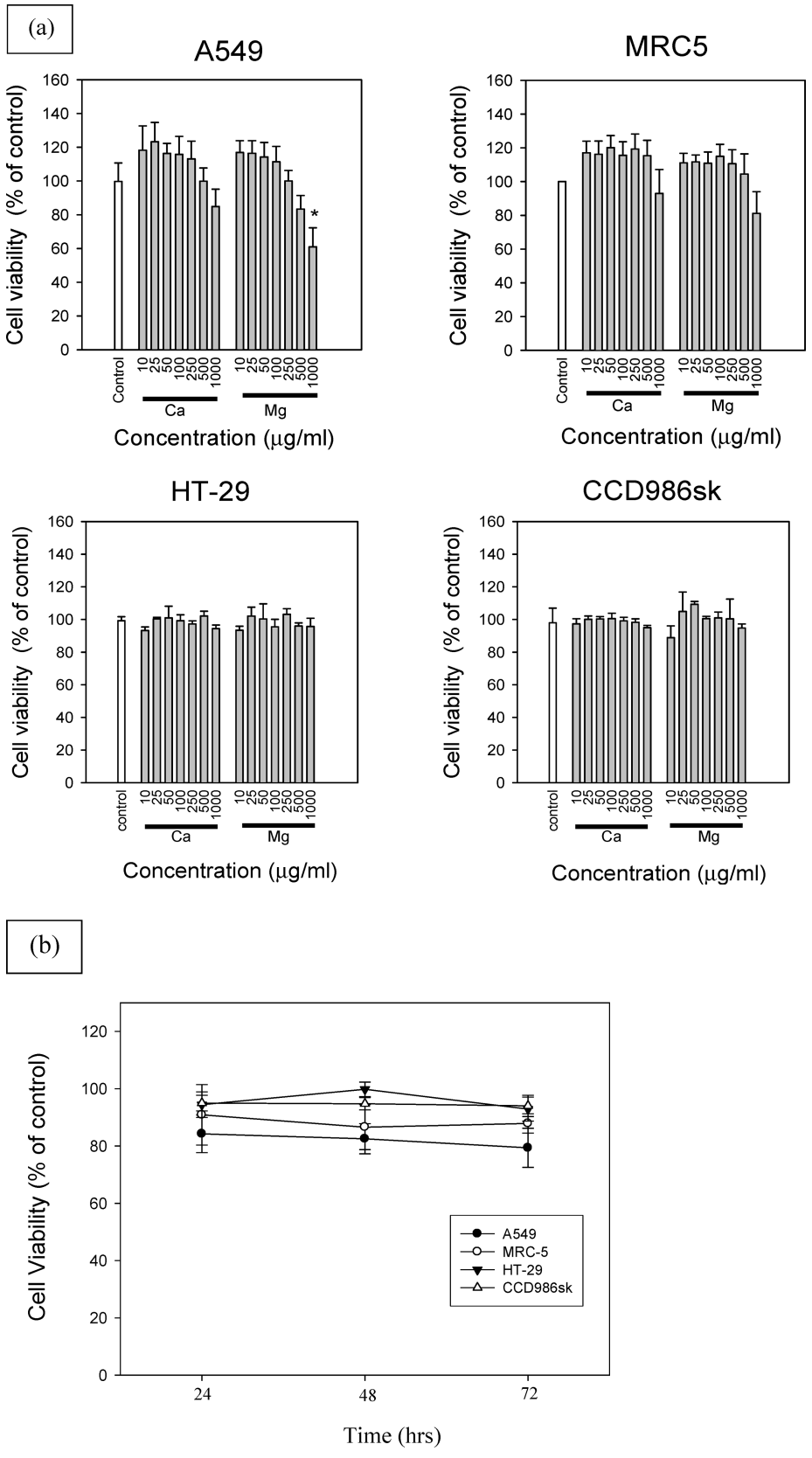

Figure 4. Effects of organoclays on cell viability. (a) Concentration-dependent cytotoxic effects of AMP and ACP clays were evaluated after a 24 h incubation. (b) Time-dependent cytotoxicity of ACP clay was assessed at a concentration of 1000 μg/mL. Cytotoxicity is expressed relative to nontreated control cells. Data are represented as means ± SD (n = 4). * $p < 0.05$ compared to the control group.

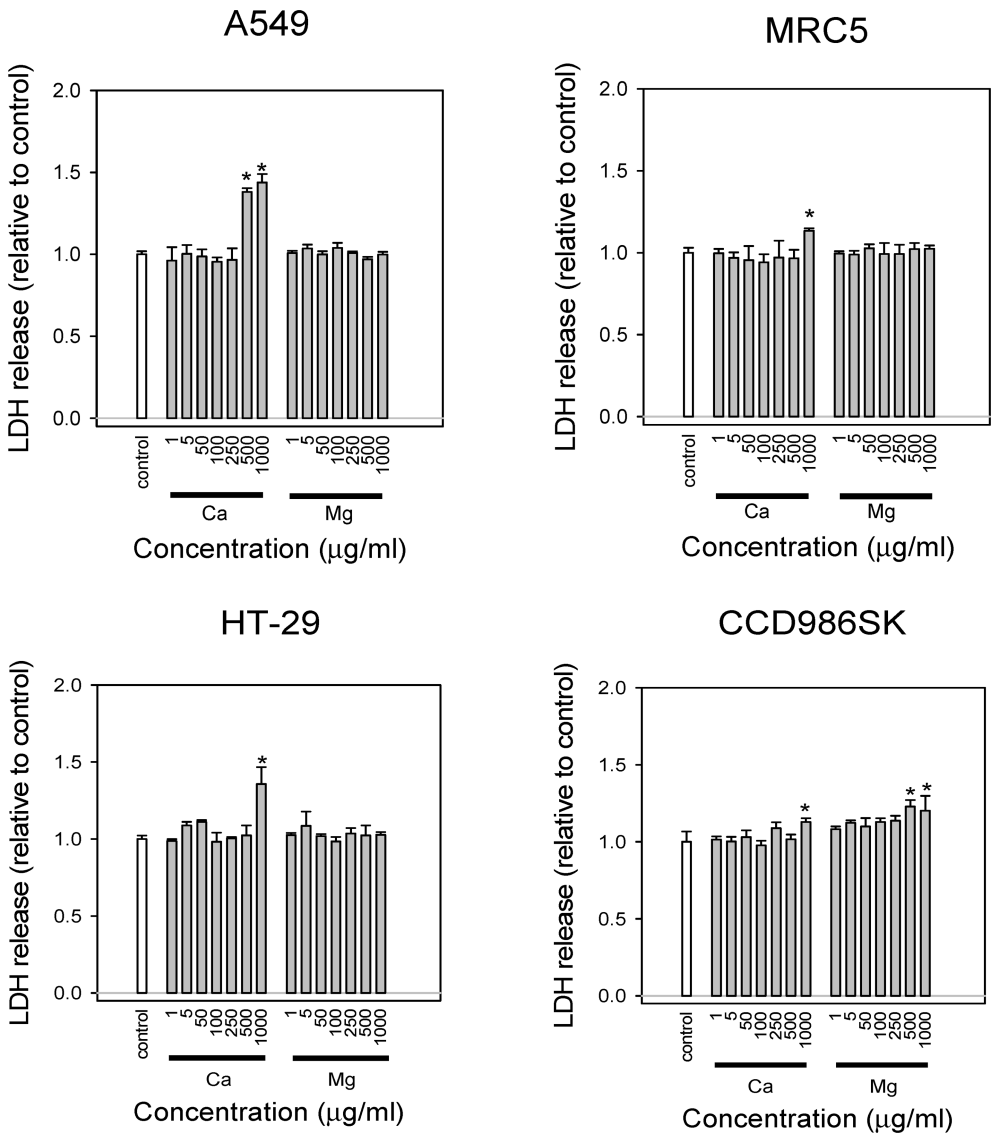

Figure 5. Effect of organoclays on membrane damage. Cytotoxicity is expressed relative to basal LDH release from control cells. Data are represented as means ± SD (n = 4). * $p < 0.05$ compared to the control group.

severe cell membrane damage in CCD986sk cells even at high concentrations. ACP clays also showed similar profiles over concentrations up to 500 μg/mL, and their toxicity was not significant. At a concentration of 1000 μg/mL, ACP clays significantly increased LDH release in all of the tested cells but to different degrees. Considering the practical concentrations of organoclays as drug delivery carriers should be below 100 μg/mL, ACP clays could not be acutely toxic at practical concentrations. In addition, the effect of ACP clays on LDH release seemed to be greater in cancer cells than in normal fibroblast cells. As indicated by previous studies,[11,12] some tumor cells, including A549 cells, appeared to be unable to tolerate exposure to nanoparticles through high metabolic activity during in vitro cytotoxicity tests. On the other hand, most human tumor cell lines are capable of maintaining their cell proliferation and membrane integrity during exposure to high dosages of nanoparticles. The greater susceptibility of cultured cancer cells to organoclays may be useful in developing delivery carriers for cancer cell targeting.

MTT and LDH measured the toxicity generated by the different mechanisms, so certain level of difference can be observed between the assays. More important thing is that MTT and LDH assays indicated that both organoclays (AMP and ACP) had little cytotoxicity in all of the cells tested at concentrations as high as 500 μg/mL and over the practically achievable concentrations, both organoclays exhibited similarly nontoxic profiles in both assays. By comparing with nanosilicate platelets (below 1000 μg/mL after 12 h incubation period),[25] organoclays induce low damage on various cell lines in both assays.

3.3. Apoptosis in A549 and MRC-5 Cells by Organoclays. The mechanisms for toxic effects are very diverse. In addition, each in vitro assay for the evaluation of toxicity is working via the different toxicity mechanisms and also has certain level of limitation. So in general, several different assays are done together to evaluate the potential toxicity of certain compounds. So we assessed apoptosis and necrosis by using the annexin V binding and propidium iodide (PI) permeability assays. One of

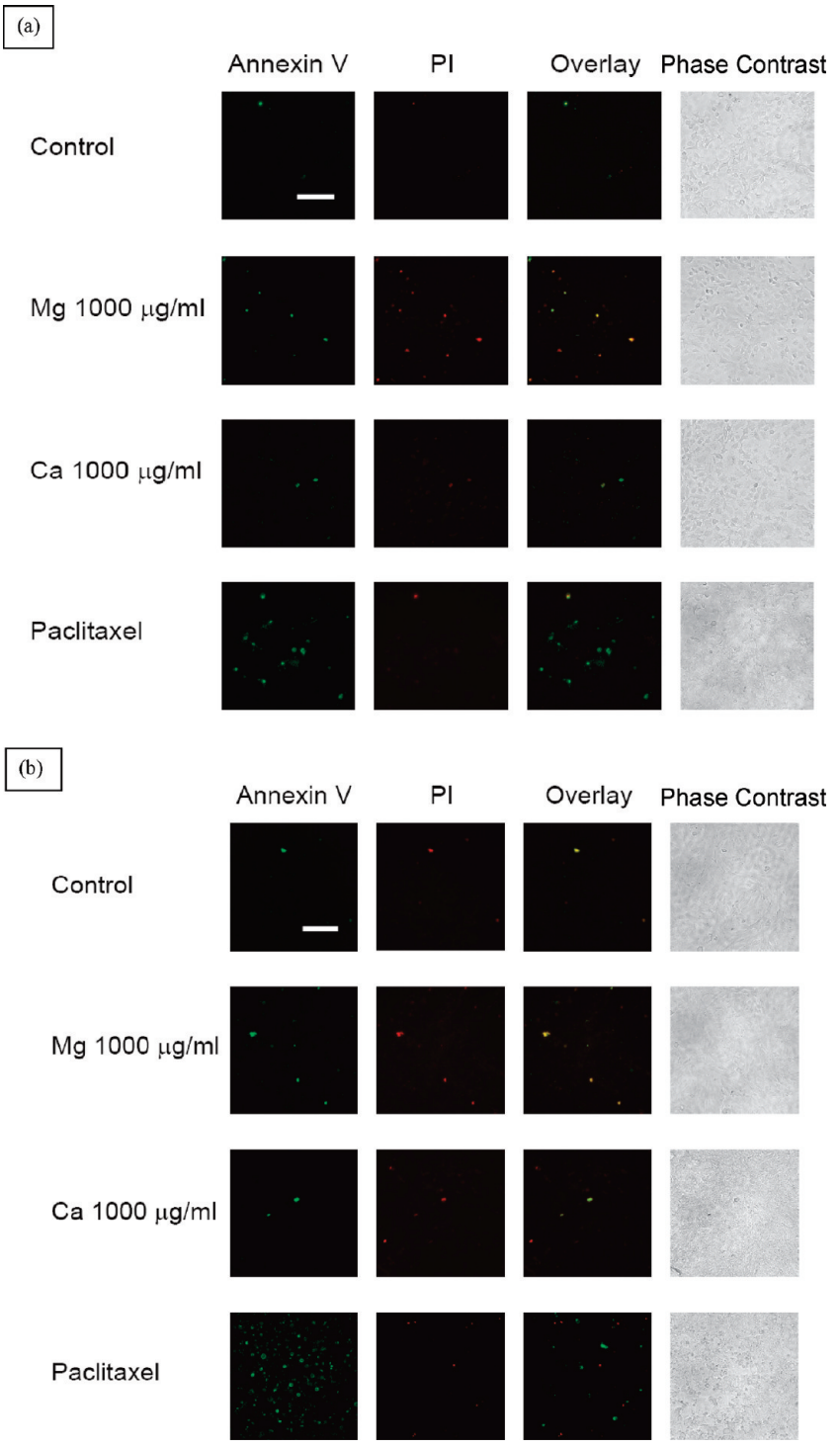

Figure 6. Apoptosis in (a) A549 and (b) MRC-5 cells. Cells were treated with organoclay for 24 h and stained with annexin V and propidium iodide (PI). Images were obtained for annexin V (green, first vertical panel), PI (red, second vertical panel) and the phase-contrast images were shown in last panel. For convenience of comparison between annexin V and PI, overlaid images were presented in third vertical panel. The positive control was treated with 1 μM paclitaxel. Images are representative of three repeated experiments. Scale bar = 150 μm.

the earliest indications of apoptosis (programmed cell death) is the translocation of the membrane phospholipid phosphatidylserine (PS) from the inner to the outer surface of the plasma membrane. Annexin V has a high affinity for PS and, thus, reveals the presence of phospholipids on the outer surfaces of cells. This event precedes the loss of membrane integrity, leading to cell death in later stages, which can be determined with PI, a membrane impermeable nucleic acid binding dye. Thus, annexin V-positive cells represent early apoptosis. Cells that are positive for both annexin V and PI are in late apoptosis or necrosis. In the present study, cells were incubated with organoclays at concentrations of 100 to 1000 μg/mL for 24 h and stained with Alexa

Fluor 488-conjugated annexin V and PI. The representative images obtained at 1000 μg/mL are presented in Figure 6 (see the Supporting Information, Figure S2 for results at lower concentrations). As illustrated in Figure 6, even at a high concentration of 1000 μg/mL, organoclays caused minimal cell death, further indicating low toxicity of organoclays. In addition, cells exposed to organoclays became both annexin V and PI positive, suggesting that they were in late apoptosis or necrosis. These data appeared to be consistent with the cell viability data obtained using the MTT and LDH assays.

As nanoparticles are used in various fields including photonics, cosmetics, pharmaceutics, and medicines, the toxic effects of nanoparticles like iron oxide, silica, and carbon nanotubes have been extensively studied in vitro and in vivo.[13,41−43] Iron oxide reduces cell viability at concentrations as low as 50 μg/mL, and silica particles cause acute pulmonary toxicity with pulmonary inflammation and tissue damage.[13,41,42] Recently, Manna et al.[43] reported that single-walled carbon nanotubes could induce oxidative stress, with a significant decrease in cell proliferation and even cell death. In contrast, the present study indicated that the potential toxicity of synthesized organoclays was low in terms of cell proliferation, membrane damage and apoptosis, even at a high concentration of 1000 μg/mL. The toxicity profile was similar between the two cations (Ca and Mg) in organoclays. Active cationic amine ($-NH_3^+$) groups of water-soluble organoclays not only increased bioavailability to cells but reduced cytotoxicity, which indicates that the density of amine groups, silica, and carbon chains has little effect on cytotoxicity, even at high concentrations. To introduce cationic amine groups with functionalities that can influence polymeric properties, cationic polymers like poly(amido amine)s have been used for the development of safe and efficient gene delivery vectors.[44]

4. CONCLUSION

In summary, host materials such as layered double hydroxides and tube-type hallosite clay[19,45,46] have been tested for toxicity and proven to be nonviral vectors for gene/drug delivery. However, to our knowledge, there are no such reports on water-soluble organoclays. Therefore, the present study suggests that organoclays might be applicable in designing and developing a novel drug carrier for controlled and targeted drug delivery with a reduction of risk to the environment and as a nontoxic host material for humans, up to a certain concentration. We are currently pursuing the detailed mechanism of organoclay interaction with cells. We are now planning in vivo and in vitro studies of drug release and delivery using these organoclays for nonviral vectors, taking into consideration the proven concept of cellular uptake of FITC-conjugated AMP clay in A549 cells in a time-dependent manner.[34]

■ ASSOCIATED CONTENT

Supporting Information. FT-IR spectra of AMP and ACP clays are shown in Figure S1. Apoptosis assays performed at various AMP clay concentrations to assess the concentration dependency in toxicity and representative images over the concentration range of 100−1000 μg/mL of organocalys are presented in Figure S2. This material is available free of charge via the Internet at http://pubs.acs.org/.

■ AUTHOR INFORMATION

Corresponding Author

*E-mail: shinhj@chosun.ac.kr. Phone: +82-62-230-7518. Fax: +82-62-230-7226.

■ ACKNOWLEDGMENT

This research was supported by the Pioneer Research Center Program through the National Research Program of Korea funded by the Ministry of Education, Science and Technology (Grant No. 2008-2000122).

■ REFERENCES

(1) Ruiz-Hitzky, E.; Ariga, K.; Lvov, Y. In *Bio-inorganic Hybrid Nanomaterials: Strategies, Syntheses, Characterization and Applications*; Patil, A. J., Mann, S., Eds.; Wiley-VCH: Weinheim, Germany, 2008; Vol. 8, p 239.
(2) Mann, S. *Nat. Mater.* **2009**, *8*, 781.
(3) Paiva, L. B.; Morales, A. R.; Díaz, F. R. V. *Appl. Clay Sci.* **2008**, *42*, 8.
(4) Fonseca, M. G.; Airoldi, C. *Thermochim. Acta* **2000**, *359*, 19.
(5) Lagadic, I.; Mitchell, M. K.; Payne, B. D. *Environ. Sci. Technol.* **2001**, *35*, 984.
(6) Visera, C.; Cerezo, P.; Sanchez, R.; Salcedo, I.; Aguzzi, C. *Appli. Clay. Sci.* **2010**, *48*, 291.
(7) Holmström, S. C.; Patil, A. J.; Butler, M.; Mann, S. *J. Mater. Chem.* **2007**, *17*, 3894.
(8) Nel, A.; Xia, T.; Mädler, L.; Li, N. *Science* **2006**, *311*, 622.
(9) Lewinski, N.; Colvin, V.; Drezek, R. *Small* **2008**, *4*, 26.
(10) Martin, C. R.; Kohli, P. *Nat. Rev. Drug Discov.* **2003**, *2*, 29.
(11) Chang, J. S.; Chang, K. L. B.; Hwnag, D. F.; Kong, Z. L. *Environ. Sci. Technol.* **2007**, *41*, 2064.
(12) Lin, W.; Huang, Y. W.; Zhou, X. D.; Ma, Y. *Toxicol. Appl. Pharmacol.* **2006**, *217*, 252.
(13) Berry, C. C.; Wells, S.; Charles, S.; Aitchison, G.; Curtis, A. S. *Biomaterials* **2004**, *25*, 5405.
(14) Wagner, S.; Münzer, S.; Behrens, P; Scheper, T.; Bahnemann, D.; Kasper, C. *J. Phys. (Paris)* **2009**, *179*, 012022.
(15) Xia, T.; Kovochich, M.; Liong, M.; Mädler, L.; Gilbert, B.; Shi, H.; Yeh, J. I.; Zink, J. I.; Nel, A. E. *ACS Nano* **2008**, *2*, 2121.
(16) Chang, E.; Thekkek, N.; Yu, W. W.; Colvin, V. L.; Drezek, R. *Small* **2006**, *2*, 1412.
(17) Keenan, C. R.; Goth-Goldstein, R.; Lucas, D.; Sedlak, D. L. *Environ. Sci. Technol.* **2009**, *43*, 4555.
(18) Brunner, T. J.; Wick, P.; Manser, P.; Spohn, P.; Grass, R. N.; Limbach, L. K.; Bruinink, A.; Stark, W. J. *Environ. Sci. Technol.* **2006**, *40*, 4374.
(19) Vergaro, V.; Abdullayev, E.; Lvov, Y. M.; Zeitoun, A.; Cingolani, R.; Rinaldi, R.; Leporatti, S. *Biomacromolecules* **2010**, *11*, 820.
(20) Ghosh, P. S.; Kim, C.-K.; Han, G.; Forbes, N. S.; Rotello, V. M. *ACS Nano* **2008**, *2*, 2213.
(21) Isobe, H.; Tanaka, T.; Maeda, R.; Noiri, E.; Solin, N.; Yudasaks, M.; Iijima, S.; Nakamura, E. *Angew. Chem., Int. Ed.* **2006**, *45*, 6676.
(22) Lopez, A. I.; Reins, R. Y.; McDermott, A. M.; Trautner, B. W.; Cai, C. *Mol. Biosyst.* **2009**, *5*, 1148.
(23) Kolhatkar, R. B.; Kitchens, K. M.; Swaan, P. W.; Ghandehari, H. *Bioconjugate Chem.* **2007**, *18*, 2054.
(24) Lee, C.-C.; Liu, Y.; Reineke, T. M. *Bioconjugate Chem.* **2008**, *19*, 428.
(25) Li, P.-R.; Wei, J.-C.; Chiu, Y.-F.; Su, H.-L.; Peng, F.-C.; Lin, J.-J. *ACS Appl. Mater. Interfaces* **2010**, *2*, 16083.
(26) da Fonseca, M. G.; Airoldi, C. *J. Chem. Soc., Dalton Trans.* **1999**, 3687.
(27) Burkett, S. L.; Press, A.; Mann, S. *Chem. Mater.* **1997**, *9*, 1071.

(28) Mann, S.; Burkett, S. L.; Davis, S. A.; Fowler, C. E.; Mendelson, N. H.; Sims, S. D.; Walsh, D.; Whilton, N. T. *Chem. Mater.* **1997**, *9*, 2300.
(29) Patil, A. J.; Muthusamy, E.; Mann, S. *Angew. Chem., Int. Ed.* **2004**, *43*, 4928.
(30) Patil, A. J.; Muthusamy, E.; Mann, S. *J. Mater. Chem.* **2005**, *15*, 3838.
(31) Patil, A. J.; Li, M.; Dujardin, E.; Mann, S. *Nano Lett.* **2007**, *7*, 2660.
(32) Bromley, K. M.; Patil, A. J.; Seddon, A. M.; Booth, P.; Mann, S. *Adv. Mater.* **2007**, *19*, 2433.
(33) Shamsi, M. H.; Geckeler, K. E. *Nanotechnology* **2008**, *19*, 075604.
(34) Lee, Y.-C.; Lee, T.-H.; Han, H.-K.; Go, W. J.; Yang, J.-W.; Shin, H-J. *Photochem. Photobiol.* **2010**, *86*, 520.
(35) Lagadic, I. L. *Microporous Mesoporous Mater.* **2006**, *95*, 226.
(36) Minet, J.; Abramson, S.; Bresson, B.; Sanchez, C.; Montouillout, V.; Lequeux, N. *Chem. Mater.* **2004**, *16*, 3955.
(37) *CytoTox 96R non-radioactive cytotoxicity assay technical bulletin*, part TB 163, 10 revised 9/04; Promega Cooperation: Madison, WI, 2004; p 5371.
(38) Hillegass, J. M.; Shukla, A; Lathrop, S. A.; MacPherson, M. B.; Fukagawa, N. K.; Mossman, B. T. *Wiley Interdiscip. Rev. Nanomed. Nanobiotechnol.* **2010**, *2*, 219.
(39) Sohaebuddin, S. K.; Thevenot, P. T.; Baker, D.; Eaton, J. W.; Tang, L. *Part. Fibre Toxicol.* **2010**, *7*, 22.
(40) Lordan, S; Kennedy, J. E.; Higginbotham, C. L. *J. Appl. Toxicol.* **2011**, *31*, 27.
(41) Carrero-Sanchez, J. C.; Elías, A. L.; Mancilla, R.; Arrellín, G.; Terrones, H.; Laclette, J. P.; Terrones, M. *Nano Lett.* **2006**, *6*, 1609.
(42) Jia, G.; Wang, H.; Yan, L.; Wang, X.; Pei, R.; Yan, T.; Zhao, Y.; Guo, X. *Environ. Sci. Technol.* **2005**, *39*, 1378.
(43) Manna, S. K.; Sarkar, S.; Barr, J.; Wise, K.; Barrera, E. V.; Jejelowo, O.; Rice-Ficht, A. C.; Ramesh, G. T. *Nano Lett.* **2005**, *5*, 1676.
(44) Lin, C.; Engbersen, J. F. J. *J. Controlled Release* **2008**, *132*, 267.
(45) Richard-Plouet, M.; Vilminot, S.; Guillot, M.; Kurmoo, M. *Chem. Mater.* **2002**, *14*, 3829.
(46) da Fonseca, M. G.; Silva Filho, E. C.; Machado Junior, R. S. A.; Arakaki, L. N. H.; Espinola, J. G. P.; Airoldi, C. *J. Solid State Chem.* **2004**, *177*, 2316.